Spectral filtering of visible light by the cuticle of metallic woodboring beetles and microfabrication of a matching bioinspired material

Jean Pol Vigneron,[1,*] Marie Rassart,[1] Cédric Vandenbem,[1] Virginie Lousse,[1,2] Olivier Deparis,[1] László P. Biró,[3] Daniel Dedouaire,[4] Alain Cornet,[4] and Pierre Defrance[4]

[1]*Laboratoire de Physique du Solide, Facultés Universitaires Notre-Dame de la Paix, rue de Bruxelles, 61, B-5000 Namur Belgium*

[2]*Ginzton Laboratory, Stanford University, Stanford, California 94305, USA*

[3]*Research Institute for Technical Physics and Materials Science, P. O. Box 49, H-1525 Budapest, Hungary*

[4]*Unité de Physique Atomique, Moléculaire et d'Optique, Université Catholique de Louvain, Chemin du Cyclotron, 2, B-1348 Louvain-la-Neuve Belgium*

(Received 17 October 2005; revised manuscript received 30 January 2006; published 7 April 2006)

Samples of the cuticle taken from the body of Buprestidae *Chrysochroa vittata* have been studied by scanning electron microscopy and optical reflectance measurements, related to numerical simulations. The cause of the metallic coloration of the body of these insects is determined to be the structure of the hard carapace constructed as a stack of thin chitin layers separated by very thin irregular air gaps. In particular the change of color as a function of the observation angle is elucidated in terms of an infinite photonic-crystal model, confirmed by finite multilayer calculations. These mechanisms are used to develop an artificial bioinspired multilayer system which reproduces the visual effects provided by the insect surface.

DOI: 10.1103/PhysRevE.73.041905 PACS number(s): 87.68.+z, 42.70.Qs, 42.66.−p, 42.81.Qb

I. INTRODUCTION

Buprestidae (Coleoptera) is a large and well known family of insects. In their adult phase, they often show a very tough and brightly colored carapace, which explains the common name of "metallic woodboring beetles" often given to some of them. They live on trees, bushes, and herbaceous plants and can be found almost everywhere in the world, although their frequency increases in hot and sunny tropical regions. The larvae usually spend their lives boring wood or bark of trunks, logs, branches, and roots. As a consequence, they are generally considered noxious to agriculture and, especially, arboriculture.

This family of insects is particularly rich in colorful specimens. Figure 1 shows one of this species, *Chrysochroa vittata*, which bears essentially green elytrons (i.e., the hard protective cover which hides the insect's wings). The coloration of Buprestidae is sometimes associated with camouflage, but, in the case of these brightly colored species, the visual effects may rather aim at contrasting with other Coleoptera, so that they can recognize their own species from other interacting organisms in their neighborhood. It could also be that these insects partially rely on their sense of vision to improve on the number of mating opportunities. With few exceptions (for instance the black *Melanophila* or *Merimna*) this makes Buprestidae typical diurnal species. Slight variations of coloration allow one to distinguish between very closely related species, and in some genera, allow one to differentiate males and females.

From the physical point of view, the vivid coloration resulting from the sharp filtering reflectance is not the only interesting characteristic of these beetles. The metallic finish of the cuticle surface is another important fact, related to the strict specularity of the light reflection process. Also, a most important and spectacular feature, for which a biological functionality is harder to discover, is the fact that the hue of the reflection changes drastically as the angle of incidence is changed from normal to grazing. The displacement of the reflection to shorter dominant wavelengths can easily be seen by naked eyes, for instance on the insect's back which (for *Chrysochroa vittata*) appears green under normal incidence, and blue under a grazing view. On the other side, the ventral segments of the abdomen appear red under normal incidence, and show a bluish green under grazing angles. In many Coleoptera, these features are related to a layered structure of the exocuticle [1] and, as we will see below, this will be no exception here.

The physical origin of the coloration of insects was suspected very early [2,3] and directly confirmed by electron microscopy as soon as this technique was made available [4].

FIG. 1. (Color online) The large family of insects known as Buprestidae possesses many vividly colored members. *Chrysochroa vittata*, shown here, is special in that its body displays a metallic green finish, which turns blue under large incidences. The ventral part (hidden) of the abdomen is red under normal incidence, but shifts to green under large angles. Picture by Daniel Van Acker.

*Electronic address: jean-pol.vigneron@fundp.ac.be

Since then, one- [5], two- [6], and even three-dimensional [7] photonic crystals have been shown to be responsible for the coloration of many living organisms [8]. The precise measurement of reflectance spectra, scanning and transmission electron microscopy, and detailed numerical simulations, used as cooperative tools, have often been instrumental in understanding the engineering of photonic devices put to work in biological organisms. With precisely the same techniques, this paper will focus on the detailed structure of the exocuticle of *Chrysochroa vittata*. More specifically, the cuticle on the ventral side of the body, visible during the insect flight, will be studied. This shows a red iridescence under normal incidence, which turns green at more grazing angles. A simple rule, based on photonic-crystal theory, is derived in order to explain the coloration changes actually observed. The modeling point of view taken in the present paper is somewhat unconventional: rather than considering the interference effect in a few layers as an extension of the single-layer interference (as usually done), we will describe these structures as part of an infinite stack of layers, thereby considering the reflectance as a consequence of the presence of a photonic stop band. This will not only provide a much simpler description of the physical mechanism, it will also indicate where the layer characteristics can be freely changed without altering the reflectance spectrum.

With this knowledge and understanding, a completely artificial layer structure is designed in order to achieve optical properties very similar to those of the Buprestis exocuticle. Achieving such a "copy" can be seen as a confirmation of the validity of the photonic-crystal interpretation of the optical response. Simple evaporation of SiO and metallic layers (not air, the photonic-crystal mechanism allows for the replacement) is used in order to produce these bioinspired layers, which were grown on various substrates. The achievement of the angular change of coloration found on the insect cuticle can readily be observed with naked eyes. Measurements compared to theoretical predictions will confirm the natural-artificial similarities.

II. SCANNING ELECTRON MICROSCOPE IMAGES OF THE INSECT CUTICLE

The cuticles of these arthropods are hard, and samples can be obtained by breaking pieces of the exoskeleton for observation. Immersion in liquid nitrogen gives a better chance of a neat fracture and eases the image interpretation. The cleaved surfaces, covered with 15 nm gold, are convenient samples for examination with a scanning electron microscope (Philips XL20 SEM).

The samples are taken from the ventral segments of the abdomen of *Chrysochroa vittata*. In this species, the ventral side of the abdomen is metallic red at normal incidence, turning to metallic green at large angles. In Fig. 2, the fracture provided an opportunity to observe the terraces left by the layered structure cleaved along an oblique angle. This picture suggests that the exocuticle structure is actually a simple planar multilayer composed by stacking chitin plates with equal thicknesses on top of each other. The thickness of these chitin plates accounts for nearly all the lattice parameters of the multilayer, so that the junction layers separating the plates must be extremely thin. From the optical point of view, this means that, though their location determines the multilayer period and thus appears crucial to determine the reflected wavelength, their actual composition and refractive index are immaterial.

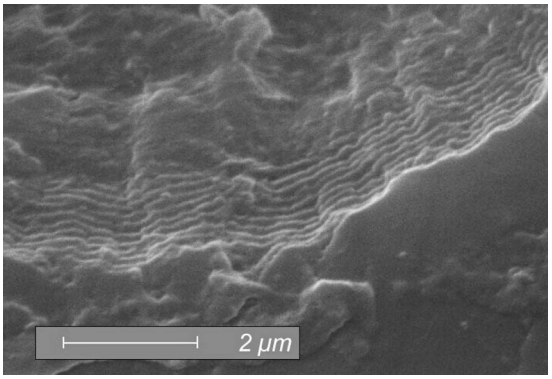

FIG. 2. The very thin layer at the surface of the cuticle of *Chrysochoa vittata* is a stack of about 20 planar slabs of chitin, with a refractive index $n_c \simeq 1.56$. The layer that separates these slabs is actually extremely thin, and thus difficult to show on this scanning electron microscope image.

Figure 3 shows the same structure in a region where the cleavage occurred in a direction normal to the surface. This disposition of the cleavage plane allows us to examine the multilayer stack from a lateral viewpoint, and is much more effective in providing quantitative geometric data on the exocuticle multilayer. About 20 layers can be observed through the filtering film, each with a thickness that can be estimated to be 204 nm. The cut is much more regular in this hard external layer than in the rest of the exoskeleton, which contains fibrous material that brings mechanical strength and resistance to the segment of the carapace.

It is plausible that the junction layer between two thick chitin plates just contains air, the spacers being provided by slight irregularities of the chitin plate surfaces. This is con-

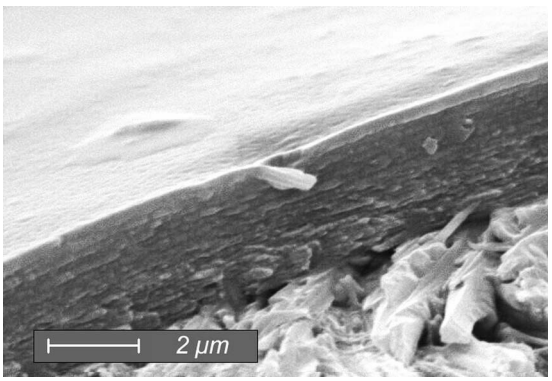

FIG. 3. Scanning electron micrograph of the outer part of the cuticle of *Chrysochroa vittata*. This very hard protective layer is a simple multilayer stack of planar sheets of chitin. The sample examined here is taken on the ventral part of the insect abdomen, which displays a red coloration when viewed from a direction normal to the upper surface.

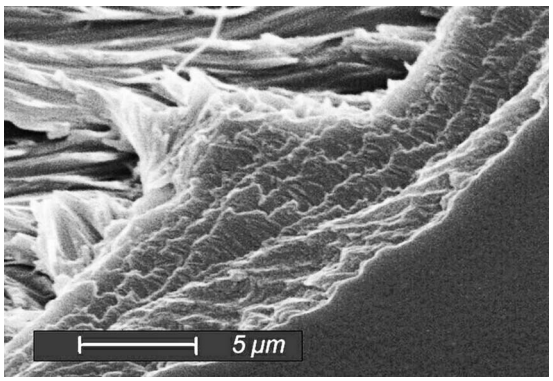

FIG. 4. (Color online) Scanning electron micrograph view of the cuticle of *Chrysochroa vittata*, broken at an angle large enough to display some of the chitin layer surface, as terraces. Irregularities can be seen on the plate surface, which, plausibly, play the role of spacers, leaving air between the plates. This allows for a periodic perturbation of the chitin bulk volume. This perturbation gives rise to the interferences responsible for the coloration of the ventral side of the body surface.

firmed by another view of the multilayer, which is shown in Fig. 4. In this view, the surface of the chitin sheets is uncovered, so that the surface irregularities are apparent. As the simple model developed later suggests, the amplitude of these irregularities determines the air spacing between the chitin sheets. The size and shape of this separation layer contribute to the reflectance bandwidth, and not to the dominant wavelength.

III. REFLECTANCE SPECTRA

The reflection spectrum from the ventral side of the abdomen of *Chrysochroa vittata* has been investigated using an Avaspec 2048/2 fiber-optic spectrometer. Measurements were performed, under 0°, 30°, and 75° incidence, in a specular geometry. The results are shown in Fig. 5. The reflected intensity is expressed in units of the corresponding diffuse reflection obtained on a standard white (Avaspec) diffusing surface (a common way of normalization which leads to the expression of a "reflection factor," not necessarily bounded by 100%).

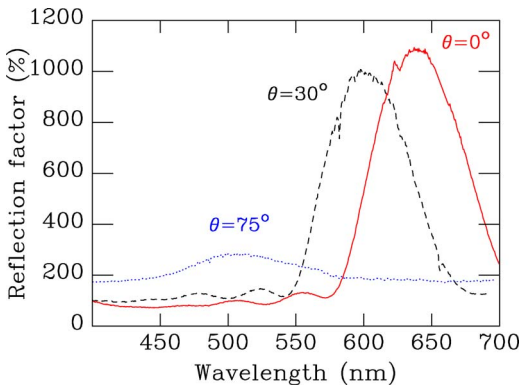

FIG. 5. (Color online) Spectrum of light reflected from the ventral side of the body of *Chrysochroa vittata* in the specular direction, for three incidence angles. The strong reflection band shifts from red to green as the angle of incidence is increased. The reflected intensity is compared to a white diffusely reflected intensity, not to the incident intensity.

The spectrum at normal incidence, restricted to the human visible range, essentially contains a single band. As seen in Fig. 5, this band is located around the central wavelength $\lambda \simeq 639$ nm, which lies in the red part of the human visible spectrum. When increasing the angle of incidence to $\theta = 30°$, the central wavelength of the reflection band shifts to $\lambda \simeq 600$ nm, in the yellow region. As the next section shows more quantitatively, this shift to a shorter wavelength is essentially related to the increase with incidence angle of the optical path of an oblique wave, if the same standing wave condition is kept on the normal wave number. The blueshift of the reflected wavelength is, as expected, more pronounced when the angle of incidence reaches the value $\theta = 75°$ (Fig. 5). For this geometry, we see the dominant wavelength reach a value as low as 505 nm, in the green spectral range.

Other parts of the body of *Chrysochroa vittata* behave with exactly the same trends. The elytrons, the hardened caps covering the flappable wings when the insect is at rest, display a vivid metallic green under normal incidence. When viewed with a large angle of incidence, for instance when looking at the animal from the rear, the green part turns to a bluish gray. All this corresponds to the behavior expected from a coherent one-dimensional photonic-crystal film built in the same way as for the ventral side of the body, except for the multilayer period, which is found significantly smaller under scanning electron microscope observation.

IV. DOMINANT REFLECTED WAVELENGTH

The analysis of the dominant wavelength reflected by a finite stack of layers is usually treated by using detailed Fresnel formulas, which can become rapidly cumbersome with just a few layers. Instead, here we suggest another approach based on an infinite multilayer with a strict periodicity (one-dimensional photonic crystal). The physics and the interpretation are significantly different from the usual descriptions, since the standing wave arguments are here replaced by the Bloch theorem, which assumes perfect lattice translational invariance. The advantage, as shown below, is the simplicity of the result, but not its generality: this formulation is essentially adapted to weak refractive index inhomogeneities, and thus is best suited to the consideration of photonic structures of biological origin.

For a regular multilayer with little refractive index contrast in the period layer, the dominant reflected wavelengths can be easily determined by the following rule, based on a "long wavelength" approximation. We consider a periodic planar multilayer stack, grown along the z direction, and interrupted by a flat surface, say, at $z=0$. The effective or metamaterial below the surface has an average refractive index $\bar{n}$ which, for transverse electric polarization, is easily determined from an arithmetic average of the dielectric response of the period contents. For a period composed of two

layers, one of thickness ℓ_1 with refractive index n_1, and a second one of thickness ℓ_2 with refractive index n_2, the average refractive index is calculated as

$$\bar{n}^2 = \frac{\ell_1 n_1^2 + \ell_2 n_2^2}{\ell_1 + \ell_2} \tag{1}$$

for transverse-electric (TE) waves, whatever the incidence. For transverse-magnetic (TM) waves, the near-normal average value is the same, but as the incidence becomes large, we should switch to another averaging scheme,

$$\frac{1}{\bar{n}^2} = \frac{\ell_1 (1/n_1^2) + \ell_2 (1/n_2^2)}{\ell_1 + \ell_2}. \tag{2}$$

These averages neglect retardation effects and are reminiscent of the parallel (TE) or series (TM, large angle) assemblies of capacitances, formed by the multilayer interfaces. In many cases, this estimation will be a sufficiently accurate starting point. The dispersion relation for light waves propagating in this averaged multilayer structure is simply

$$k = \bar{n}\frac{\omega}{c}. \tag{3}$$

This relation will be perturbed by the periodic variation of the refractive index when we will consider the slight disturbance induced by the contrast between n_1 and n_2 in the period component layers. However, owing to Bloch's theorem, only wave vectors parallel to the multilayer normal, and differing by a reciprocal lattice step, integer multiples of $2\pi/a$, will be coupled ($a = \ell_1 + \ell_2$ is the one-dimensional lattice parameter). The only wave vectors for which this occurs at the same frequency are located at the border of the Brillouin zones, at

$$k_z = m\frac{\pi}{a} \tag{4}$$

where m is an integer ($m = 1, 2, 3, \ldots$). The normal wave number in the multilayer is actually related to the wave frequency and the conserved parallel component k_y of the wave vector through the relation

$$k_z = \sqrt{\left(\bar{n}\frac{\omega}{c}\right)^2 - {k_y}^2}. \tag{5}$$

Now, if the one-dimensional photonic crystal is terminated by a surface, we can make a connection between the wave traveling in the structure and an incident wave, because the lateral wave number k_y is conserved. In air, with an incidence angle θ (angle from normal along z), this wave number is

$$k_y = \frac{\omega}{c}\sin\theta. \tag{6}$$

Finally, matching Eqs. (4)–(6), we get the stop-band formation condition

$$\frac{\omega}{c} = \frac{m\pi/a}{\sqrt{\bar{n}^2 - \sin^2\theta}} \tag{7}$$

which can be translated into vacuum wavelengths to produce the "gap" wavelengths

$$\lambda = \frac{2a\sqrt{\bar{n}^2 - \sin^2\theta}}{m}. \tag{8}$$

Total reflectances will appear at these frequencies, and these will provide the dominant wavelength which determines the coloration, according to colorimetric rules. When only one integer value m leads to a visible dominant wavelength λ, the coloration of the multilayer is readily determined.

This formula is very general, as it determines the wavelengths that must be totally reflected by an infinite multilayer, for any incidence angle, only assuming weak refractive index contrasts.

As an example, take the multilayers revealed by scanning electron microscopy for *Chrysochroa vittata*, under normal incidence. For $\theta = 0$, the dominant wavelength depends on reflectance bands described by

$$\lambda = \frac{2a\bar{n}}{m}. \tag{9}$$

For the layers seen in Fig. 3, we can estimate the thickness to be $a = 204$ nm and, at normal incidence, the average refractive index is $\bar{n} = 1.537$ in both TE and TM cases [see Eq. (1), with $\ell_1 = 194$ nm, $\ell_2 = 10$ nm, $n_1 = 1.56$, $n_2 = 1$]. The value of the visible-light chitin refractive index was taken from Ref. [9], but for the present estimations, the weak imaginary part $n_1' = 0.06$ was neglected. Only $m = 1$ gives rise to a visible reflection band, which occurs at the wavelength $\lambda = 627$ nm. This red coloration is indeed observed at normal incidence on the ventral side of the *Chrysochroa vittata*, from which the exocuticle sample was taken. When the angle of incidence is increased, the TE refractive index keeps the same value as for the normal incidence, while the TM average approaches 1.508 [see Eq. (2), with the same values of ℓ_1, ℓ_2, n_1, n_2 as above]. The term $\sin\theta$ under the radical in Eq. (8) further reduces the value of the effective refractive index, and this leads to a blueshift of the dominant wavelength. At grazing incidence (we take $\theta = 75°$ as in experiment), the present model leads to a dominant wavelength of 488 nm for the TE polarization, and 472 nm for the TM polarization. This shift is easily observed when looking at the insect from its side or rear: the ventral side of the insect's abdomen displays, to the naked eye, a bluish-green coloration. At an intermediate angle $\theta = 30°$, the reflected wavelength can be estimated to be $\lambda = 2 \times 204\ \text{nm} \times \sqrt{(1.537)^2 - (0.5)^2} = 593$ nm for TE waves (588 nm for TM waves). It should be emphasized that these results are obtained with very simple rules, based on the concept of an ideal, infinite, one-dimensional, periodic stack. However, we will see now that these estimations are fully confirmed by a more precise consideration of a finite-stack multilayer.

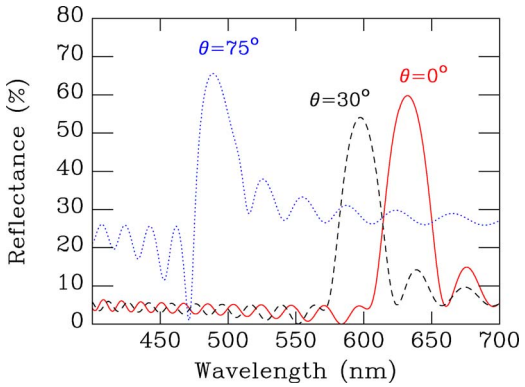

FIG. 6. (Color online) Reflectance spectra of the chitin/air multilayer, calculated from exact solution of Maxwell's equations. The system is a repetition of 20 periods (a=204 nm), each comprising a thick layer of chitin (refractive index 1.56) and a very thin (10 nm) layer of air. The reflectance is an average of TE and TM polarizations, given as a function of the incident wavelength λ. The dominant wavelength is, as expected, found to be blueshifted as the incidence angle θ is increased.

V. DETAILED MODELING

Transfer matrices can make a more complete job than the above long-wavelength rule when calculating the detailed reflectance spectra. Figure 6 shows the reflectance spectrum in the visible range for three incidence angles θ=0° (solid line), θ=30° (dashed line), and θ=75° (dotted line). In this calculation, the geometric parameters corresponding to the observed structure of the cuticle of *Chrysochroa vittata* were taken, i.e., as above, a multilayer of period a=204 nm, 194 nm of which is chitin (refractive index 1.56) and 10 nm of air. This calculation, which amounts to solve Maxwell's equations with scattering boundary conditions, is essentially exact, being amenable to reduction of a simple one-dimensional problem [10].

It is interesting to note that the value of 10 nm of air is only indicative, being difficult to measure on the electron microscope images available to us. However, the above photonic-crystal picture teaches us one thing: the reflected wavelength depends only on the multilayer period and the average refractive index. When the periodicity is induced by a very thin layer of air, the average refractive index is always close to that of chitin (the rest of the period) and the exact value of the air-layer thickness is immaterial, as well as other characteristics of this layer, such as the lateral roughness.

The dominant wavelength at normal incidence, at the maximum of the reflectance spectrum, is found to be 632 nm (very close to the estimated 627 nm predicted by the "infinite stack" of Sec. IV). This, according to a standard colorimetric classification [11], corresponds to a red perception. This red reflection is easily seen when viewing the ventral side of the *Chrysochroa vittata* body under normal incidence, with the naked eye. For an incidence angle θ=30°, we find a dominant wavelength at 597 nm, which is usually classified as orange (Sec. IV predicted 593 nm, again in good agreement). Finally, for an incidence angle θ=75°, the dominant wavelength is shifted to bluish-green, near 488 nm, with a weak shoulder just above 500 nm. [In Sec. IV, these two wavelengths correspond to TM (472 nm) and TE (488 nm) which were found for the infinite stack. The main contribution to the large calculated band is actually the band produced by reflection on the wide TE multilayer gap: the TM contribution is weaker because the multilayer gap closes at the nearby Brewster incidence, at $\theta \simeq 57°$.] At large angles (θ =75°), the overall reflection tends to be higher than for near-normal incidences: this is a grazing-reflection effect, the reflectance reaching 100%, theoretically, at 90° incidence. The results provided by the simple "averaged" model of the previous section are less than 5% off the values determined from the calculated finite-multilayer spectra.

The linewidth experimentally observed on the natural multilayer in Fig. 5 is larger than the linewidth of the calculated reflectance. The difference is attributed to the disorder shown at the level of the surface of the air layer which separates two chitin slabs in the exocuticle multilayer. This situation was also encountered with the coloring structure of *Hoplia coerulea* [8], where the broadening and "triangular" line shape could be related to some orientation disorder in the multilayer. Also, the line shape of the blue reflectance band calculated for large incidence angles does not agree with the measured spectrum as closely as could be expected. This can also be related to disorder: near normal incidence, the "lateral" wavelength, parallel to the sample surface, is large on the scale of the layer irregularities, so that the roughness is easily averaged out. This is not so at large incidences, where lateral roughness is found on the scale of the lateral wavelength.

The agreement between the full reflectance calculation and the rule (8) built from the infinite stack consolidates our understanding of the mechanism involved in the cuticle coloration. The structure is best seen as a homogeneous piece of chitin (with an average refractive index close to 1.56), in which a series of perturbative layers are introduced, parallel to the exposed surface. These layers are equidistant planes, thin enough not to change the average refractive index in any significant way. However, just their presence creates a band discontinuity at the location of the Brillouin zone boundary, and a total reflection in the associated gap. The important point is that the color produced by this reflection depends on the *distance* separating the perturbing planes and does not depend on the *nature* of the perturbing planes. This coloration mechanism is actually very robust against any change made to the material which fills the perturbing layer. In other words, the violence of the modification of the refractive index will not impact the coloration, nor its change with the incidence angle, as long as the perturbing layer is kept extremely thin. This mechanism, involving the periodic interruption of a homogeneous material by perturbing planes is different from the usual bilayer dielectric stack (with more symmetry between the layer thicknesses in the period) used to create selective mirrors, one of the advantages of the thin-layer design being precisely the insensitivity to the composition of the material that makes the perturbation. In the next section, we exploit that (bioinspired) very robust technique in order to produce the *Chrysochroa vittata* color variability in an artificial design.

VI. DESIGN AND FABRICATION OF AN ARTIFICIAL SELECTIVE SURFACE BASED ON THE *CHRYSOCHROA VITTATA* CUTICLE STRUCTURE

Confirming the understanding of the coloration process is one thing but, on the grounds of this understanding, requesting the fabrication of an artificial structure which reproduces the visual effect seen on the insect is clearly a step further. Such a color-selecting surface may have a number of uses, but this will not be the main point here.

We aim to reproduce the visual effect, but not the exact multilayer stack. Although inspiration about the actual structure to be chosen comes from the study of the natural design, which presumably results from million years of optimization, under the evolutionary pressure of collective benefits acquired from the interaction with the environment.

In order to reproduce the precise visual effect observed on *Chrysochroa vittata*, the structure is copied, with some variations which account for a mode of production very different from the natural autoassembly process. The chitin plate (refractive index 1.56) will be replaced by a layer of silicon monoxide (SiO), with a refractive index 1.9. According to the above discussion of the dominant wavelength, this calls for a reduction of the multilayer period to 180 nm, 170 nm of which will be the monoxide. For the deposition of this material, evaporation from an electrically (Joule) heated tantalum crucible was required, producing a stream of material directed toward a revolving sample.

The periodically repeated introduction of an air layer with spacers was considered much too complicated, as it would require the separate production of every period slab, with one surface appropriately etched to define the spacers. The subsequent assembly step, by a wafer fusion technique, though already well studied [12], is still a challenging approach. However, the purpose of this irregular interlayer is simply to produce a periodic perturbation in order to open the one-dimensional photonic gaps. The location (primarily, the spacing) of these perturbing planes is crucial to define the gap spectral location, but the exact nature of the perturbation is not, as long as it does not change the average refractive index in a very significant way. So the process can be simplified by replacing the roughly planar air gaps of the insect's structure by, for instance, a very thin layer of metal occupying the same positions. This perturbation would define the required periodic dielectric response, contrasting adequately with the silicon monoxide response. The deposition of metal is obtained from the evaporation of a nickel cathode, impacted by accelerated electrons driven by the static magnetic field of a permanent magnet. The complex refractive index of nickel, which slightly depends on the wavelength, can be found in the tables published by Palik [13]. At 590 nm, the complex refractive index can be written $n_{Ni}=1.85+i3.48$. The perturbation is thus brought here by the strong imaginary part of the refractive index, which defines tiny mirrors in the multilayer stack. Of course, for the same reason related to the average refractive index robustness, other metals could have been chosen, leading to the exact same color variations.

Other solutions than creating an array of metal layers could be envisioned, such as using only dielectric layers. The choice of a metal such as nickel was made on purpose: by using such a violent change of the nature (and dielectric response) of the perturbing layer (moving from an air gap to a nickel layer), we demonstrate the validity of the photonic-crystal picture, where any periodic perturbation, with the right lattice parameter, will produce the appropriate change of coloration.

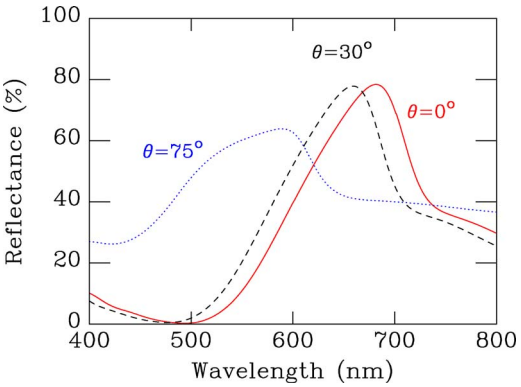

FIG. 7. (Color online) Predicted reflectance of the bioinspired structure made of silicon monoxide and nickel. This structure selectively reflects a dominant wavelength which scans a large part of the visible spectrum when the angle of incidence is changed from normal to grazing. The multilayer alternates a silicon monoxide plate 170 nm thick with a 10 nm nickel spacer layer.

In order to confirm the demonstrative value of our design, the optical behavior can be checked by reflectance calculations. In the simulation reported in Fig. 7, the number of layers is, at the same time, economized, the structure being designed as a stack of only six two-layer periods. One layer is a 170 nm thick silicon monoxide plate, with a refractive index 1.9 (i.e., a dielectric constant $\varepsilon=3.61$), and a second is a 10 nm thick nickel film. The whole multilayer is assumed to be deposited, metal first, on a (theoretically) flat glass substrate. The results in Fig. 7 have been obtained, assuming planar layers and averaging over TE and TM polarizations, from a one-dimensional transfer-matrix calculation [10]. The dispersive nickel layers are thick enough to induce changes of the line shape of the reflected band, which becomes asymmetric. As expected, the strong modification of the junction layer does not qualitatively affect the specifically targeted optical property: a blueshift (from red) of the dominant reflected wavelength is still clearly predicted with the increase of the angle of incidence (from normal). This confirms that the air-to-metal substitution is permitted, as expected, but also that the infinite-stack reflectance is already adequately reproduced with a small number of periods.

The actual realization of this structure provided artificial square glass plates 15 cm along each edge. As seen in Fig. 8, the coloration of the plate closely matches that of the insect abdomen, even when the angle of incidence is changed.

The measurement of the spectral reflectance of the plate provides more details on the wavelengths filtering upon reflection. Figure 9 shows the reflected intensity (again in terms of a white diffusive standard) for three incidence angles $\theta=0$, $\theta=30°$, and $\theta=75°$. These measurements confirm that the spectral content of the light reflected from the plates accurately reproduces the exocuticle reflectance. The

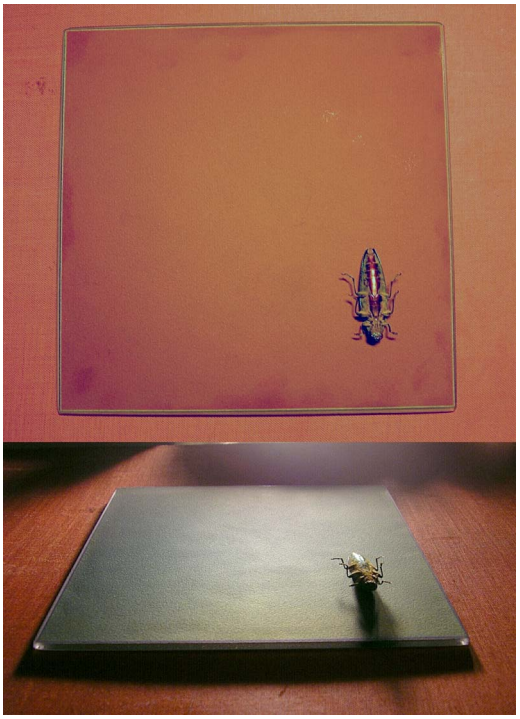

FIG. 8. (Color online) The artificial surface and the ventral segments of the carapace of *Chrysochroa vittata*, viewed together under two incidences. Under normal incidence (above), the surface reflects red light, while under a larger incidence angle (below), the coloration turns to green.

dominant wavelengths agree with the original values measured on the insect to within 10% (702 nm under normal incidence, 662 nm when θ=30°, and 495 nm when θ=75°). Note that measured spectra show a "reflection factor" (normalized to a white diffusive standard) while calculated spectra are reflectances in the proper sense.

Compared to theoretical calculations, the measured spectrum is also broadened. A basic difference is the surface roughness. The calculation assumed a flat, planar substrate surface, while in the realized structure, the substrate is sand blasted glass. The surface roughness can be seen on the scale revealed by the optical microscope. The deposited multilayer thickness is defined at a smaller scale, so that the deposition can be considered to be made on a surface whose orientation is spatially fluctuating. This again leads to uncertainties on the value of the incidence angle. The associated fluctuations of the reflectance spectrum explain the reflection band broadening.

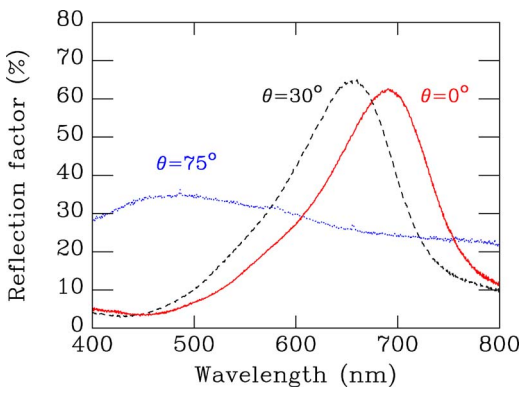

FIG. 9. (Color online) Measured reflected intensities from the surface of the artificial iridescent plate fabricated to match the optical properties of the beetle *Chrysochroa vittata*. The dominant wavelength sweeps a large part of the visible spectrum when the angle of incidence is varied.

VII. CONCLUSION

In this paper, the multilayer structure producing the coloration of a specimen belonging to the family of Buprestidae has been investigated, by a combination of scanning electron microscopy, reflectance measurements, theoretical modeling, and numerical simulations. The physical origin of the coloration is a stop band in a one-dimensional photonic crystal made as a stack of chitin plates. These plates have a rough surface, with weak protrusions which act as spacers, so that very thin air layers appear, equidistantly distributed, with a period of about 204 nm. This gives weak periodic perturbations which open gaps in the mode dispersion relations at the one-dimensional Brillouin zone boundaries, explaining the reflectance bands responsible for the coloration at normal incidence. In the framework of the same model, the blueshift of the dominant wavelength can also be explained. The optical properties of a coleopter like *Chrysochroa vittata* can be easily understood on the basis of these mechanisms.

The knowledge acquired in performing this study has been used to develop an artificial surface which reproduces the visual effect found with the insect cuticle. A multilayer alternating thick silicon monoxide plates and thin nickel layers has been designed with the aim of providing the same visible light filtering as the ventral segments of the insect. In this multilayer, normal incidence leads to a red reflectance, while higher angles lead to yellow and green colorations. This correctly matches the optical behavior of some parts of the exocuticle of *Chrysochroa vittata*. It should be noted that, compared to more classical dielectric mirrors, where the layers in the periods have optical paths of, roughly, the same order of magnitude, the present multilayer is much more dissymmetric: it can be viewed as homogeneous material, in which extremely thin perturbative layers are periodically introduced. The advantage, exploited by the natural structure, is the insensitivity of the reflectance band spectral location to the nature of the thin perturbing layer. This is demonstrated in the fact that the selective surface targeted properties are conserved when changing the rough air gap into a smoother metal layer. On one hand, this shows the robustness of the optical properties of the insect cuticle, as produced by millions of years of evolution. On the other hand, this robustness allows us to envision rather free adaptations when designing the artificial structure.

Iridescent panels could find many uses in the hands of object designers. For a long time, parts of the body of metallic woodboring beetles have been added as decorative elements on clothes, furniture, or even walls and ceilings. They have also been incorporated in various artworks, playing a role similar to valuable pieces of jewelry. One of the most

famous uses of the cuticle of a beetle for visual effects is perhaps the decoration of the Japanese Tamamushi-no-Zushi, an altar conserved in the Houryuu-ji temple, at some distance from the ancient town of Nara, in Japan. 1300 years ago, this altar was decorated with elytrons taken from about 2600 beetles. The Japanese ''tamamushi,'' a Buprestidae correctly named *Chrysochroa fulgidissima* [14], used in this decoration, is a very close relative of the insect studied in the present work. Using real living organisms for decoration, as is done nowadays by contemporary artists (see for instance the recent restoration of one of the rooms of the Royal Palace in Brussels), may not be advisable from the naturalist's point of view. Using artificial materials is certainly a welcome alternative. The craftsmen in Sendai (again in Japan) may have been aware of this when they introduced the Tamamushi-nuri lacquer coat, a hard surface treatment of wood requiring the application, by hand, of up to 50 layers of a special lacquer, separated by thin films of metal dust. As the name of the technique indicates, this beautiful finish is claimed to resemble the iridescent tamamushi, and, in particular, the purple stripe on its back. Interestingly, the present work could perhaps be regarded as a more technological (and maybe more faithful) version of this ancient traditional know-how.

ACKNOWLEDGMENTS

This investigation was conducted with the support of the European NEST STREP BioPhot project, under Contract No. 12915 and support from EU5 Centre of Excellence ICAI-CT-2000-70029 [Inter-University Attraction Pole (IUAP P5/1) on "Quantum-Size Effects in Nanostructured Materials" of the Belgian Office for Scientific, Technical, and Cultural Affairs]. The use of Namur Interuniversity Scientific Computing Facility (Namur-ISCF) is acknowledged. This work has also been partly supported by the European Regional Development Fund (ERDF) and the Walloon Regional Government under the "PREMIO" INTERREG IIIa project. V.L. and C.V. were supported by the Belgian National Fund for Scientific Research (FNRS). The authors from UCL acknowledge financial support from the "Institut Interuniversitaire des Sciences Nucléaires" (IISN-FNRS). We thank Daniel Van Acker, from the Audio-Visual and Electronics Services of the University of Namur, for supplying the picture of *Chrysochroa vittata* in Fig. 1.

[1] S. Berthier, *Iridescences, Les Couleurs Physiques des Insectes* (Springer-Verlag, Paris, 2003).
[2] Lord Rayleigh, Philos. Mag. **37**, 98 (1918).
[3] Lord Rayleigh,Proc. R. Soc. London, Ser. A **103**, 233 (1923).
[4] K. Gentil, Z. Morphol. Oekol. Tiere **38**, 344 (1942).
[5] C. G. Bernhard, G. Gemne, and A. R. Moeller, Quart. Rev. Biophys. **1**, 89 (1968).
[6] J. Zi, X. Yu, Y. Li, X. Hu, C. Xu, X. Wang, X. Liu, and R. Fu, Proc. Natl. Acad. Sci. U.S.A. **100**, 12576 (2003).
[7] A. R. Parker, V. L. Welch, D. Driver, and N. Martini, Nature (London) **426**, 786 (2003).
[8] J. P. Vigneron, J.-F. Colomer, N. Vigneron, and V. Lousse, Phys. Rev. E **72**, 061904 (2005).
[9] P. Vukusic, J. Sambles, C. Lawrence, and R. Wootton, Proc. R. Soc. London, Ser. B **266**, 1403 (1999).
[10] A. Dereux, J. P. Vigneron, P. Lambin, and A. A. Lucas, Phys. Rev. B **38**, 5438 (1988).
[11] R. S. Berns, *Billmeyer and Saltzman's Principles of Color Technology*, 3rd ed. (Wiley-Interscience, New York, 2000).
[12] S. Noda, K. Tomoda, N. Yamamoto, and A. Chutinan, Science **289**, 604 (2005).
[13] E. D. Palik, *Handbook of Optical Constants of Solids* (Academic Press, Boston, 1985).
[14] T. Hariyama, M. Hironaka, H. Horiguchi, and D. G. Stavenga, in *Structural Colors in Biological Systems, Principles and Applications*, edited by S. Kinoshita and S. Yoshioka (Osaka University Press, Osaka, 2005).